© 2016. Published by The Company of Biologists Ltd | Journal of Experimental Biology (2016) 219, 3981-3987 doi:10.1242/jeb.147124

RESEARCH ARTICLE

Three-dimensional motion tracking reveals a diving component to visual and auditory escape swims in zebrafish larvae

Benjamin H. Bishop, Nathan Spence-Chorman and Ethan Gahtan*

ABSTRACT

Escape behaviors have been studied in zebrafish by neuroscientists seeking cellular-level descriptions of neural circuits but few studies have examined vertical swimming during escapes. We analyzed three-dimensional swimming paths of zebrafish larvae during visually-evoked and auditory-evoked escapes while the fish were in a cubical tank with equal vertical and lateral range. Visually evoked escapes, elicited by sudden dimming of ambient light, consistently elicited downward spiral swimming (dives) with faster vertical than lateral movement. Auditory taps also elicited rapid escape swimming with equivalent total distance traveled but with significantly less vertical and more lateral movement. Visually evoked dives usually ended with the zebrafish hitting the bottom of the 10 cm^3 tank. Therefore, visually evoked dives were also analyzed in a tubular tank with 50 cm of vertical range, and in most cases larvae reached the bottom of that tank during a 120 s dimming stimulus. Light-evoked spiral diving in zebrafish may be an innate defense reflex against specific predation threats. Since visual and auditory escapes are initially similar but dives persist only during visual escapes, our findings lay the groundwork for studying a type of decision-making within zebrafish sensorimotor circuits.

KEY WORDS: Zebrafish, Escape, Reflex, Swimming

INTRODUCTION

Neuroscientists have long studied escapes and other defensive reflexes in simple model organisms (Domenici et al., 2011a,b), including zebrafish (Eaton and Emberley, 1991; Kimmel et al., 1974), because the stereotyped movements suggest dedicated and relatively simple mechanisms. Goals of studying escape-related swimming in zebrafish have included investigating the synaptic structure of sensorimotor circuits (Gahtan et al., 2002; Portugues and Engert, 2009; Stobb et al., 2012) and genetic regulation of circuit development (Fleisch and Neuhauss, 2006; Hirata et al., 2013), among others. The presence of many identifiable neurons in zebrafish has also enabled a 'circuit busting' approach associated with classical invertebrate neuroethology (Bullock, 1975; Marder and Abbott, 1995; O'Malley et al., 2003) that seeks to reveal complete circuits for innate behaviors as well as general principles of neural circuit organization.

Neuroethologists emphasize the importance of measuring behavior in ways that meaningfully correspond to its natural expression (ecological validity) (Tinbergen, 1951). In contrast to this, most escape or startle response studies in zebrafish have measured behavior in environments that restrict vertical movement and have tracked swimming two-dimensionally with a single camera above or below the tank. This limitation is apparent in reviews of zebrafish behavioral assays (Budick and O'Malley, 2000; Champagne et al., 2010; Fleisch and Neuhauss, 2006; Mirat et al., 2013) and in tools designed for automated tracking of zebrafish behavior (ZebraLab, ViewPoint; Fontaine et al., 2008). While detailed kinematic information can be obtained from 2D imaging, such as speed, latency, direction and frequency of swimming movements, a restriction in vertical range can be a confound in locomotor assays (Zhu and Weng, 2007) and leaves open the question of whether vertical swimming would occur as part of the 'natural' behavior. Recordings of neural activity have been used in conjunction with analyses of swimming movements to study escape circuits in zebrafish, including recent advances made by measuring the lateral direction of escape tail movements during optical calcium imaging of neurons in the brain (Dunn et al., 2016; Temizer et al., 2015). These and other neural recording methods have elucidated mechanisms of lateral movement control in zebrafish (Kohashi and Oda, 2008; Gabriel et al., 2009; Knogler and Drapeau, 2014), but the need to partially or fully immobilize the animal limits the potential to detect vertical movements.

If vertical swimming were part of the normal escape responses, understanding its kinematic properties would be a first step in investigating how neurons in the brain may control vertical movement. To that end, we analyzed 3D swimming paths during visual and auditory escapes in zebrafish larvae using a two-camera imaging system and a 10 cm^3 tank with equal vertical and lateral movement range. Visually evoked vertical swimming was also tested in a 50 cm high tubular tank to better assess the distance and duration of vertical movements.

MATERIALS AND METHODS

All procedures were approved by the Humboldt State University Animal Care and Use Committee (IACUC). Embryos were obtained from mating crosses of wild-type adults of the AB/TU zebrafish (*Danio rerio* Hamilton 1822) strain that were maintained as brood stock (sex of embryos was not determined). Adults were maintained and larvae raised under standard laboratory conditions (Matthews et al., 2002). Larvae were raised in 60 mm Petri dishes (maximum 40 larvae per dish) containing approximately 25 ml of egg water at a depth of 1 cm. Larvae were tested individually during the light phase of the light–dark cycle between ages 6 and 12 days post-fertilization (dpf).

In the first experiment, the tank was a 10 cm acrylic cube (Fig. 1A). Two adjacent walls were coated with white plastic to provide contrast for imaging by two video cameras facing them (Pixelink PL-B 741, each with a Computar 12 mm, F1.4 lens fitted with a visible light blocking, infrared-pass filter and positioned 30 cm away from the tank). The tank was contained within a sound-

Department of Psychology, Humboldt State University, 1 Harpst Street, Arcata, CA 95521, USA.

*Author for correspondence (ethan.gahtan@humboldt.edu)

E.G., 0000-0001-9881-8246

Received 2 August 2016; Accepted 13 October 2016

Journal of Experimental Biology (2016) 219, 3981-3987 doi:10.1242/jeb.147124

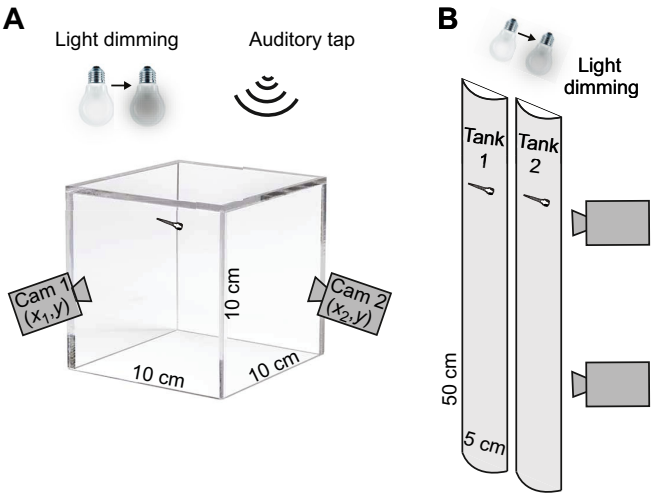

Fig. 1. Schematics of the experimental apparatus. (A) A cubical tank was used in the first experiment to avoid biasing swimming direction by affording equal vertical and lateral ranges for motion. Placement of sensory stimuli and cameras are shown, as described in the text. The views from both cameras were integrated to reconstruct 3D swimming paths. (B) The tubular tanks were used to record vertical swimming during light-dimming while allowing for greater vertical swimming range. The two cameras were used to expand the vertical imaging range, not for 3D tracking, and only vertical swimming was analyzed in these experiments.

and light-attenuating cabinet and illuminated with diffused infrared light to allow for video imaging in the dark. Visual escapes were elicited by sudden dimming of visible light lasting 60 s. The light source was an array of 20 white light LEDs arranged in a 4×5 grid (2.5×3 cm) producing about 440 lx at the recording tank, and it pointed toward the tank from 30 cm directly above. Auditory escapes were elicited by repeated tapping (at 1 Hz) of a mechanical motor 20 cm above the tank, lasting 60 s. Cameras recorded swimming movements at 1 Hz frame rate for 60 s before the stimulus and then 60 s during the stimulus period. Eight trials were run: four 'dim' and four 'tap'. Stimulus order was counterbalanced with half of the subjects receiving tap-dim-dim-tap (repeated twice) and half receiving dim-tap-tap-dim (repeated twice). An *a priori* power analysis determined that 10 larvae were needed to achieve a statistical power of 0.8, but 12 larvae were actually tested. Larvae exhibiting buoyancy and normal swimming activity, indicating an inflated swim bladder and good health, were selected randomly from the home dish. The 12 larvae were from four separate mating crosses and the data were compiled over four repetitions of the experiment. Stimulus presentation and image acquisition was controlled by a custom computer program written in DaqFactory (Azeotech) and with a LabJack U3 (LabJack Corporation) for computer hardware interface. A 60 min delay was included before trials began to allow larvae to acclimate to the new tank.

After observing escape trials in which fish reached the bottom of the 10 cm^3 tank early in the trial, we performed a second experiment with a separate group of larvae to examine vertical swimming in a tank with more (50 cm) vertical range (Fig. 1B). Tubular tanks were constructed by bisecting a 50 cm length of 5-cm-diameter PVC pipe and gluing the edges and bottoms of each half-pipe to a plate of glass (positioned side by side to form two tanks). The two cameras were positioned vertically to allow the entire vertical range of each testing tank to be imaged. Each larva (N=5) was given three dimming trials with 30 min between trials (three trials had to be discarded because of recording errors, so 12 trials were analyzed). Two minutes of post-stimulus swimming were recorded (1 Hz frame rate) on each trial. The apparatus was enclosed in a sound- and light-attenuating cabinet and video imaging used infrared illumination.

Data analysis

The x,y coordinates corresponding to the larvae's position were manually extracted for each video frame from each camera using the point tool in ImageJ (Abramoff et al., 2004). Experimenters were blinded to the larval identification code and the stimulus condition during data scoring. In the cubical tank experiments, the larvae's position in 3D space on each frame was defined by the x coordinate value from each camera (x_1, x_2) and a y coordinate that was the mean of the y values from each camera (the two y values were always nearly identical because the larva's vertical position appeared the same when viewed through either side of the tank; Fig. 1A). Microsoft Excel was used to calculate kinematic metrics and generate graphs. Values obtained in pixel units were first converted to millimeters (in our images, 1 pixel equaled 0.18 mm). The formula used to calculate total distance traveled was:

$$\sqrt{[x_{1(2)} - x_{1(1)}]^2 + [x_{2(2)} - x_{2(1)}]^2 + [\bar{y}_{(2)} - \bar{y}_{(1)}]^2}, \quad (1)$$

where subscripted numbers in parentheses indicate the relative video frame. Horizontal distance was calculated with the same formula but omitting the y coordinate. Since the directionality of vertical movement was of interest, vertical distance was calculated so that upward movements yielded positive distance values and downward movements yielded negative values, using the formula: $[\bar{y}_{(2)} - \bar{y}_{(1)}] - 1$. Total vertical distance was calculated by first converting vertical movement scores to their absolute values and then summing so the distance value accumulated whether swimming was up or down. In contrast, vertical displacement was the sum of raw vertical movement values and measured the change in vertical location within the tank over time. These location coordinates were used in MATLAB to generate 3D line plots of the movement path during each trial.

Repeated measures ANOVAs were used to analyze the effects of sensory stimuli (light dimming or auditory taps) on four swimming activity metrics: total distance, horizontal distance, vertical distance and vertical displacement. One set of analyses assessed the effects of each stimulus type by comparing activity during the stimulus with activity during an equal amount of time immediately before the stimulus. This established an independent variable, referred to as stimulus time, with two levels: before (spontaneous activity) and during the stimulus. Three, post-stimulus time bins were examined: the entire 60 s during which the stimulus was on, or just the first and last 10 s time bins. This was done to assess changes in swimming patterns during the course of the stimulus while limiting the number of time bins, and hence statistical degrees of freedom, to analyze. Another set of analyses directly contrasted stimulus type (dim versus tap) by comparing the amount of change from spontaneous swimming between the two stimuli (using the same three time bins). All statistical analyses were performed using SPSS (v.22.0.0.0). The data met ANOVA requirements for normal distribution and equal variances. For light-evoked swimming in the tubular tanks, descriptive statistics are presented for vertical distance and displacement during the 120 s post-stimulus period. Raw data, SPSS analysis files, and custom MATLAB code is available on the Open Science Framework website at https://osf.io/3eyjr/.

Journal of Experimental Biology (2016) 219, 3981-3987 doi:10.1242/jeb.147124

RESULTS

Total swimming distance

There was no main effect of sensory stimulation on total swimming distance traveled over 60 s, $F_{1,11}$=0.579, P=0.463, partial η^2=0.050. The total distance traveled within each 60 s measurement period was 331±76 mm before dimming, 301±60 mm during diming, 341±86 mm before taps and 317±82 mm after taps. Therefore, across all conditions, total swimming within 60 s was fairly consistent and averaged about 1 body length (5 mm) s^{-1}. There was also no interaction between stimulus type and stimulus time when analyzing the entire 60 s trial, $F_{1,11}$=0.045, P=0.836, partial η^2=0.004. In contrast, total distance traveled during the first 10 s of stimulation was significantly greater than spontaneous swimming, $F_{1,11}$=32.59, P<0.001, partial η^2=0.748, and distance traveled during the last 10 s of stimulation was significantly lower than spontaneous swimming, $F_{1,11}$=12.540, P=0.005, partial η^2=0.533. Dim and tap stimuli had similar effects, both causing an initial swimming activity increase and a later decrease below baseline (Fig. 2A).

Horizontal swimming distance

Mean (±s.e.m.) horizontal swimming distance significantly decreased during the 60 s stimulation period, $F_{1,11}$=6.24, P=0.030, partial η^2=0.362 from 319±70 mm to 267±57 mm for dimming and from 324±77 to 303±79 mm for auditory taps (Fig. 2B). There was no main effect of stimulus type, $F_{1,11}$=1.40, P=0.262, partial η^2=0.113, and no interaction between the two variables, $F_{1,11}$=1.16, P=0.305, partial η^2=0.095. While horizontal swimming decreased overall during stimulation, it was significantly elevated during the first 10 s of stimulation, $F_{1,11}$=22.91, P=0.001, partial η^2=0.676, for both stimuli. Horizontal distance during the last 10 s of stimulation was significantly lower than baseline, $F_{1,11}$=20.32, P=0.001, partial η^2=0.649, with a main effect of stimulus type, $F_{1,11}$=6.27, P=0.029, partial η^2=0.363, and an interaction, $F_{1,11}$=6.06, P=0.032, partial η^2=0.355, showing that dimming suppressed horizontal activity more than taps at the end of the trial (Fig. 2B).

Vertical swimming

Total vertical swimming distance in 60 s was 78.2±37.6 mm (mean±s.e.m.) before dimming, 117.8±30.1 mm during dimming, 88.6±48.8 mm before taps, and 69.4±22.5 mm during taps. There was no main effect of stimulus time $F_{1,11}$=2.00, P=0.185, partial η^2=0.154, but there was a main effect of stimulus type, $F_{1,11}$=14.99, P=0.003, partial η^2=0.577. *Post hoc* analyses showed that vertical swimming was significantly elevated during light dimming, $F_{1,11}$=16.98, P=0.002, partial η^2=0.607, but was not affected by taps, $F_{1,11}$=3.01, P=0.111, partial η^2=0.215 (Fig. 2C). When analyzing only the first 10 s of stimulation, there was a main effect of stimulus time, $F_{1,11}$=55.89, P<0.001, partial η^2=0.836, and an interaction showing that vertical activity was elevated to a greater degree during dimming (8.8±5.5 mm pre-dim and 25.4±9.1 mm during dimming) than taps (11.3±7.3 mm pre-tap and 20.8±7.2 mm during taps), $F_{1,11}$=9.33, P=0.011, partial η^2=0.459. During the last 10 s of stimulation, vertical swimming was still elevated on dimming trials (9.7 mm above baseline) $F_{1,11}$=40.30, P<0.001, partial η^2=0.786, but not on tap trials (2.1 mm below baseline), $F_{1,11}$=1.124, P=0.312, partial η^2=0.093 (Fig. 2C).

Vertical displacement

Vertical displacement, calculated by adding distance values for upward movements and subtracting for downward movement, was greater on dim than on tap trials (Fig. 3). Mean (±s.e.m.) vertical displacement across 60 s of the stimulus was −55±3.1 mm for dimming and −16±1.8 mm for taps. Both dimming and taps significantly increased negative vertical displacement across the full 60 s trial, $F_{1,11}$=31.54, P<0.001, partial η^2=0.741, and during the first 10 s, $F_{1,11}$=49.22, P<0.001, partial η^2=0.817. Dimming had a larger effect on vertical displacement as shown by a stimulus type by stimulus time interaction, $F_{1,11}$=5.24, P=0.043, partial η^2=0.323. Vertical displacement during the last 10 s of the stimulus was not significantly different from spontaneous swimming for either stimulus (evident in the displacement difference between the 50 s and 60 s time points in Fig. 3). Cumulative vertical displacement, which is equivalent to the larva's depth in the 100-mm-deep tank at

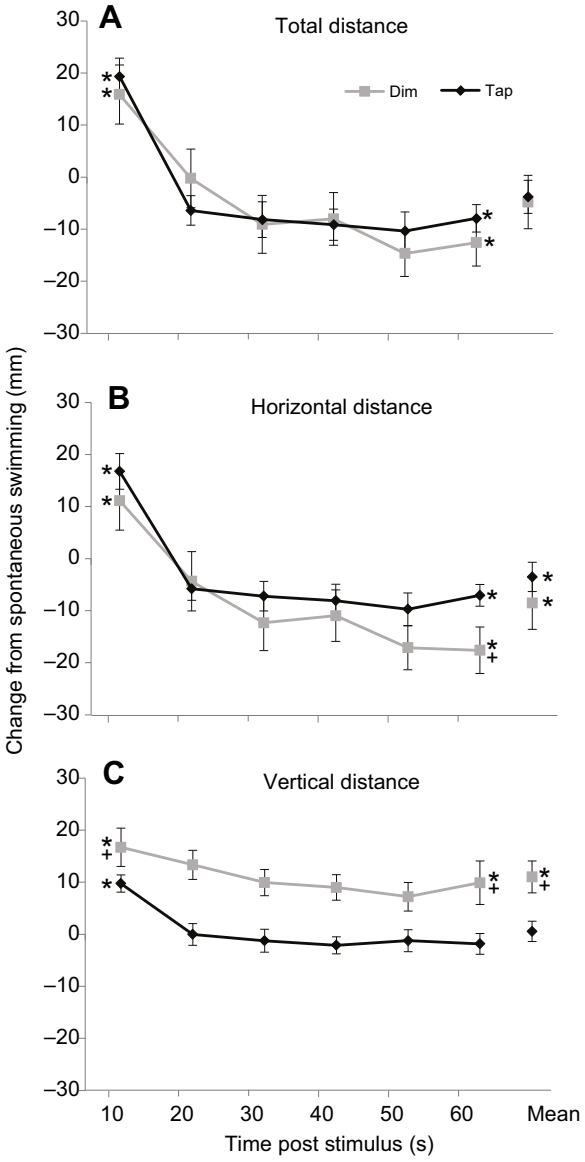

Fig. 2. Changes in vertical, horizontal and total swimming during sensory stimulation. Baseline swimming activity is normalized to zero on the *y*-axis and measurements of total swimming distance (A), horizontal-only distance (B) and vertical-only distance (C) shown over 60 s for dim and tap trials. The difference from baseline (mean±s.e.m) is shown for each 10 s time bin and for the overall mean across the 60 s trial (N=12). Positive and negative values correspond to elevation and suppression, respectively, in swimming activity. *P<0.05 between baseline and stimulation activity levels (tested only for the first 10 s, last 10 s, and for overall activity). +P<0.05 between dim and tap responses.

Journal of Experimental Biology

Journal of Experimental Biology (2016) 219, 3981-3987 doi:10.1242/jeb.147124

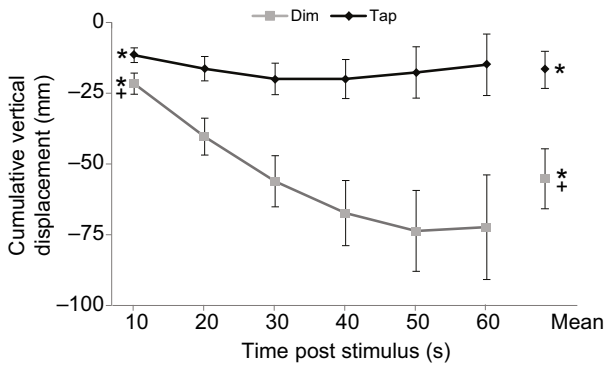

Fig. 3. Cumulative vertical displacement during sensory stimulation. Cumulative vertical displacement (mean±s.e.m), equivalent to the larva's depth position in the 100-mm-deep tank is shown at each time bin along with the mean value across the 60 s dim and tap trials. *P<0.05 between dim and tap trials (tests done only for first and last time bins and for overall mean values; N=12).

the end of the trial, averaged −72±4.2 mm on dimming trials and −14.7±1.78 mm on tap trials (60 s time point in Fig. 3).

Movement paths

Descriptive analysis of 3D movement paths during each trial is shown in Fig. 4. On most trials, spontaneous swimming (pre-stimulus) occurred toward the top of the tank. During dimming, swimming paths often appeared as a downward-oriented zig-zag from each camera (Fig. 4A) and as a downward corkscrew in 3D plots (Fig. 4B). Swimming paths during taps appeared more variable overall, lacked a consistent corkscrew pattern, and were less likely to reach the tank bottom (Fig. 4C). There was no clear directional bias for the initial escape turn. The initial escape turn direction (to the left or right as viewed from each camera) was to the left on 48% of dim trials (31 out of 64 turns) and to the left on 42% of tap trials (27 out of 64 turns).

Average vertical displacement across 120 s of dimming in the 50-cm-deep tubular tank was −305±131 mm or ∼60% of the vertical range of the tank (Fig. 5). The average rate of vertical movement was −2.5 mm s^{-1} and the maximum rate was −13 mm s^{-1} (about 3 body lengths s^{-1}). Most of these swimming paths had a downward zig-zag pattern from the single camera's view (not shown).

DISCUSSION

The current study showed that zebrafish larvae's swimming responses to visual and auditory startle stimuli include a negative vertical component, or 'dive.' This is noteworthy because escape behaviors, and their underlying neural mechanisms, have been studied in zebrafish, but usually in ways that focus on lateral and not vertical movement (Nair et al., 2015). This concern is not relevant to all studies of zebrafish escape swimming. For example, studies that focus on the role of the Mauthner neuron in escapes may ignore the potential for vertical movement because the Mauthner axon directly activates contralateral motor neurons causing a single body bend in the lateral plane (Fetcho, 1986; Korn and Faber, 2005). Nair et al. (2015) also found no vertical movement (change in pitch) during the initial C-bend in zebrafish larva escapes elicited by a water current but showed that significant changes in pitch and elevation did occur during the second and subsequent body bends and led to escape trajectories with vertical displacement (Nair et al., 2015). Therefore, neural control models of escape swim trajectory should incorporate vertical movement elements from the point of the initial body bends of an escape. Our results extend this by showing that escape-related vertical movement can persist for at least 120 s under some stimulus conditions, suggesting that vertical control neurons, about which little is currently known, have a major impact on overall motor output during visually evoked escapes. Since the initial dive maneuver is made in both visual and auditory responses, but persists only in visual responses, our findings also lay the groundwork for studying a type of sensorimotor decision-making in zebrafish.

A study by Fernandes et al. (2012) was the first to describe light-dimming-evoked dive responses in zebrafish larvae. As in the current study, light dimming produced vigorous downward swimming and increased total swimming activity immediately after the stimulus. Surprisingly, this was shown in 'blind' larvae that lack eyes or pineal photoreceptors, leading to the conclusion that the response is mediated independently of the retinotectal system. Several differences in the vertical swimming patterns described by Fernandes et al. (2012) and those reported here, however, suggest they are distinct motor responses. Although the larvae were the same approximate age when tested, we observed much faster dives, with −72±4.2 mm of vertical displacement over 60 s of dimming (∼72% of the tank's vertical range) versus about 10 mm (∼33% of the vertical range of the tank used in that study). This may reflect the loss of visual input from retinotectal pathways to premotor neurons, including the Mauthner neuron, which activate large-angle, high velocity turns at the onset of visual escapes (Temizer et al., 2015). In separate experiments where only lateral swimming was measured, these blind larvae did lack the large-angle turns, termed O-bends, normally seen upon dimming (Fernandes et al., 2012). There was no report of whether these slower dives in the blind larvae had a spiral or zig-zag form, so it is not clear whether retinotectal pathways are required to initiate that distinctive motor pattern. Another difference was the duration of increased motor output during diming, which lasted up to 6 min in the blind larvae (measuring lateral movements in a 'flat' container; Fernandes et al., 2012) but lasted only 10 s in the current experiment (measuring the 3D movement path). This difference may relate to the much lower baseline rate of swimming in the blind larvae and also points to a general difference in locomotor behavior in those larvae. Nevertheless, our study corroborates the dimming-evoked dive response reported by Fernandes et al. (2012).

The initial dimming-induced hyperactivity has been described previously as a nondirectional 'light-seeking' behavior that serves to keep larvae in brighter areas of its environment (Burgess and Granato, 2007; Fernandes et al., 2012). However, a localized looming shadow stimulus (a dark circle that rapidly expands in size) elicits strongly directional escape swims; looming shadows presented to one side activate contraversive turns, and shadows presented from the front or back activate escapes with higher or lower initial turn angles, respectively (Temizer et al., 2015). The looming shadow stimulus, which is a better approximation than whole-field brightness changes of natural visual input preceding an aerial predator strike, was also shown to activate specific retinotectal pathways, suggesting a hardwired circuit for directional responses to sudden localized dimming. Our stimuli were not localized in the lateral plane but nevertheless elicited a downward directional response. We predict that a lateralized looming shadow presented in a cubical tank would combine these navigational reflexes and elicit an initial, Mauthner neuron-mediated lateral turn away from the stimulus (Temizer et al., 2015) followed by a spiral dive and then a period of decreased swimming. The persistent hyperactivity previously reported during dimming (Burgess and Granato, 2007)

Journal of Experimental Biology

Journal of Experimental Biology (2016) 219, 3981-3987 doi:10.1242/jeb.147124

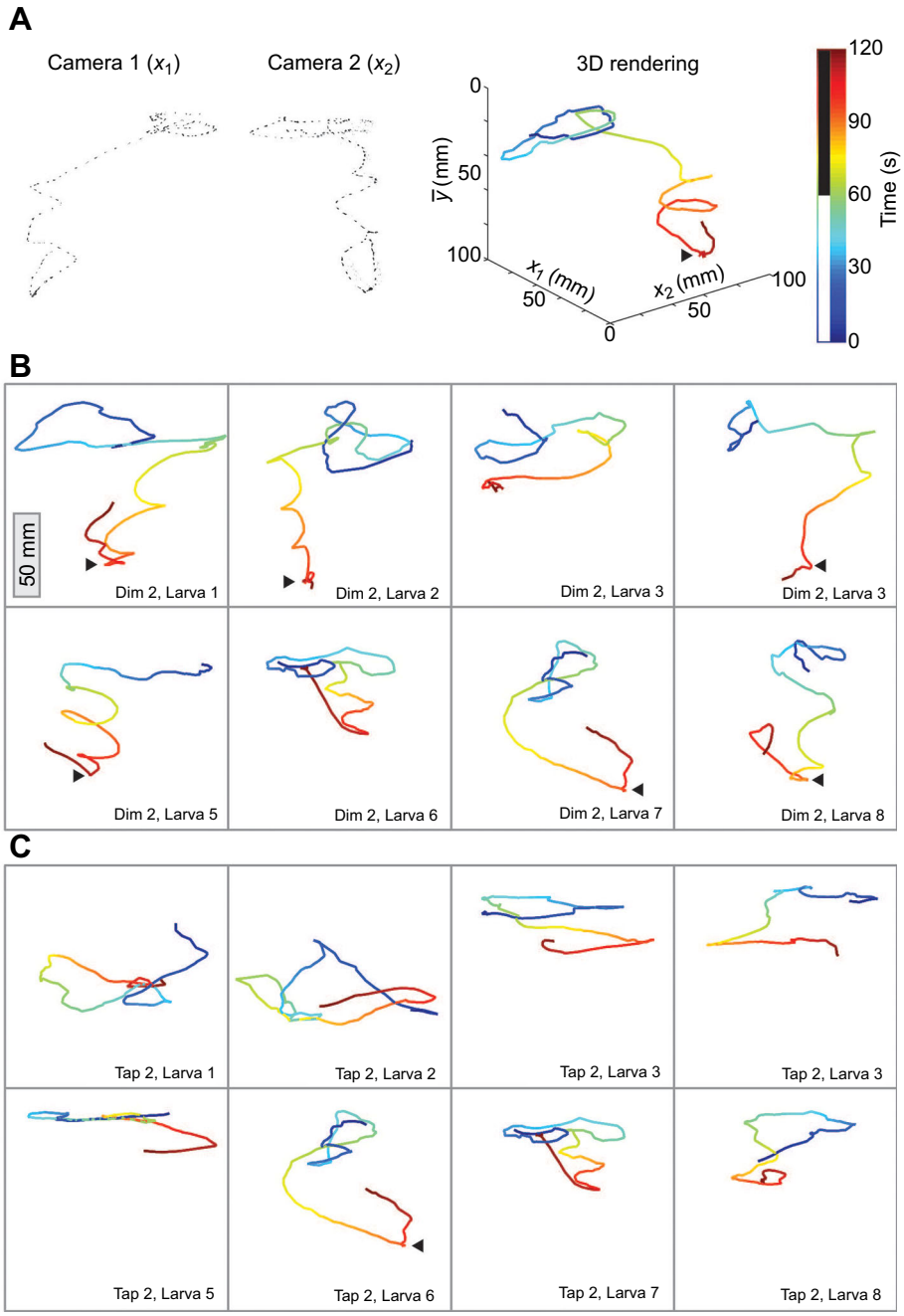

Fig. 4. Descriptive analysis of swimming paths. (A) An example of a dim trial. The left and middle panels show views from each camera. Each panel is a maximum projection of 120 images (1 s^{-1} over the 2 min dimming trial), assembled after subtracting the background on each frame to highlight the larva. The right panel shows a 3D rendering of the same trial. The color bar indicates time and the white and black bars indicate the period of pre-stimulus spontaneous swimming and the stimulus period, respectively. (B) Example 3D paths on dim trials. The second of four dim trials is shown for all eight larvae for which 3D path renderings were analyzed. The 3D axis scales shown in A apply to the individual plots, and an approximate scale bar is also shown within the first box. The colorimetric time code from A also applies. Arrowheads indicate where larvae were determined to have touched the tank bottom. (C) Tap trials (the second of four tap trials in the same eight larvae).

may reflect larvae attempting to perform such a 3D maneuver in a shallow tank.

Ethological perspectives

A possible explanation for dimming-evoked spiral dives in zebrafish is that it is an effective evolved response against aerial predators. Zebrafish mainly reside in slow-moving shallow streams and still pools where water is clear (Parichy, 2015), and remain towards the surface of the water where their prey (larval and adult insects) is most visible (Colwill and Creton, 2011), but where risk from predators is high. Kingfisher and heron both prey upon zebrafish (Parichy, 2015). Therefore, in natural environments, a sudden shadow may predict a predation strike from overhead, and the responses that have been documented, including an initial turn away from the shadow (Temizer et al., 2015) and a spiral dive in which vertical and horizontal location are continually varying, are successful techniques for evasion (Domenici et al., 2011b). In contrast, the decrease in overall swimming activity late in these escape trials is unlikely to relate to a defensive reflex, since swimming activity still seemed too great (Fig. 2A) to evade detection by predators using visual motion cues.

Implications for understanding neural mechanisms of motor control

In most fish, neural circuits in the spinal cord can maintain a simple locomotor rhythm, but modulating spinal motor circuits to produce changes in swimming speed or direction requires input from the brain. Spinal motor circuits are directly controlled by a diverse population of ‘descending’ neurons in the brain, including reticulospinal neurons (Bretzner and Brownstone, 2013), which have been studied extensively in zebrafish (Kinkhabwala et al., 2011; Stobb et al., 2012). It is likely that specific subsets of

Journal of Experimental Biology

Journal of Experimental Biology (2016) 219, 3981-3987 doi:10.1242/jeb.147124

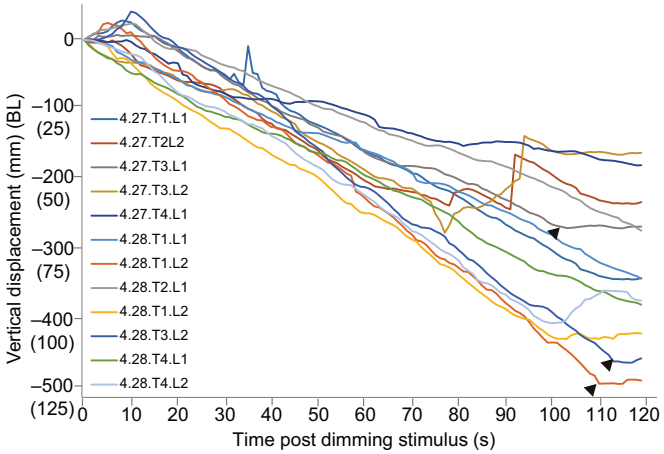

Fig. 5. Vertical displacement for all 12 dimming trials, in four different larvae, in the 50-cm-deep tubular tank. Starting position was not controlled but was normalized to zero for plotting. Arrowheads indicate when larvae were determined to have touched the tank bottom. Number of body lengths (BL) is indicated in parentheses on *y*-axis. The key shows trial identification codes.

descending neurons control vertical swimming direction by coordinating activity of dorsal and ventral muscles to alter the body's pitch angle (upward or downward), while lateral body bends provide propulsion. The current study offers several ideas for identifying descending neurons involved in vertical movement control. Since diving was sustained during visual but not auditory stimulation, recordings from descending neurons during dimming may show areas of activation not present during auditory stimulation. Utilizing genetically encoded calcium indicators (Lütcke et al., 2010; Muto et al., 2013) is a promising method for such studies in zebrafish since large numbers of neurons (in principle, the entire population of descending neurons) can be measured simultaneously.

Information about the morphology, neurotransmitter phenotype, and connectivity of descending neurons can also guide functional hypotheses that could be tested using lesion methods, as was done by Temizer et al. (2015) in experiments that ablated the Mauthner cell (a reticulospinal neuron known to receive retinotectal input through its ventral dendrite) to reveal its role in visual escape turns. In zebrafish larvae, lasers have been used to ablate individual descending neurons (Severi et al., 2014) and lesion methods linked to gene expression have been used to silence molecular classes of descending neurons (Del Bene et al., 2010). Descending neurons have diverse axon branching patterns, including unilateral or bilateral outputs and collaterals restricted to anterior, posterior, dorsal or ventral spinal areas (Gahtan et al., 2005). Descending neurons controlling downward pitch in lamprey appear to have bilateral spinal outputs that activate ventral body muscle contractions (Zelenin et al., 2007), a finding that provides another lead for identifying vertical swimming control neurons in zebrafish. The fact that these dive responses occurred reliably and with a consistent spiral swimming pattern in naïve larval fish, suggests that the neural mechanisms mediating the response are hardwired to some degree and are discoverable through the types of studies discussed above.

Although 3D motion tracking is significantly more complex than 2D tracking, some semi-automated methods exist (Stewart et al., 2015; Zhu and Weng, 2007), and custom systems can be developed as described here. Greater use of vertical motion analysis in studies of zebrafish motor control would increase ecological validity and may promote new ideas for how descending neurons control spinal circuits and locomotor movement.

Acknowledgements
We thank Dr Elizabeth Whitchurch for assistance with the MATLAB code and Dr Brad Ballinger for assistance with calculating movement parameters.

Competing interests
The authors declare no competing or financial interests.

Author contributions
All authors contributed to writing the manuscript. E.G. initiated the study. B.H.B. conducted the experiments and analyzed data. N.S.-C. analyzed data.

Funding
None of the authors, nor the research itself, received any specific grant from any funding agency in the public, commercial or not-for-profit sectors.

Data availability
Raw data, SPSS analysis files and custom MATLAB code is available on the Open Science Framework website at https://osf.io/3eyjr/.

References

Abramoff, M. D., Magalhães, P. J. and Ram, S. J. (2004). Image processing with ImageJ. *Biophotonics Int.* **11**, 36-42.
Bretzner, F. and Brownstone, R. M. (2013). Lhx3-Chx10 reticulospinal neurons in locomotor circuits. *J. Neurosci. Off. J. Soc. Neurosci.* **33**, 14681-14692.
Budick, S. A. and O'Malley, D. M. (2000). Locomotor repertoire of the larval zebrafish: swimming, turning and prey capture. *J. Exp. Biol.* **203**, 2565-2579.
Bullock, T. H. (1975). Are we learning what actually goes on when the brain recognizes and controls? *J. Exp. Zool.* **194**, 13-33.
Burgess, H. A. and Granato, M. (2007). Modulation of locomotor activity in larval zebrafish during light adaptation. *J. Exp. Biol.* **210**, 2526-2539.
Champagne, D. L., Hoefnagels, C. C. M., de Kloet, R. E. and Richardson, M. K. (2010). Translating rodent behavioral repertoire to zebrafish (*Danio rerio*): relevance for stress research. *Behav. Brain Res.* **214**, 332-342.
Colwill, R. M. and Creton, R. (2011). Locomotor behaviors in zebrafish (*Danio rerio*) larvae. *Behav. Processes* **86**, 222-229.
Del Bene, F., Wyart, C., Robles, E., Tran, A., Looger, L., Scott, E. K., Isacoff, E. Y. and Baier, H. (2010). Filtering of visual information in the tectum by an identified neural circuit. *Science* **330**, 669-673.
Domenici, P., Blagburn, J. M. and Bacon, J. P. (2011a). Animal escapology II: escape trajectory case studies. *J. Exp. Biol.* **214**, 2474-2494.
Domenici, P., Blagburn, J. M. and Bacon, J. P. (2011b). Animal escapology I: theoretical issues and emerging trends in escape trajectories. *J. Exp. Biol.* **214**, 2463-2473.
Dunn, T. W., Gebhardt, C., Naumann, E. A., Riegler, C., Ahrens, M. B., Engert, F. and Del Bene, F. (2016). Neural circuits underlying visually evoked escapes in larval zebrafish. *Neuron* **89**, 613-628.
Eaton, R. C. and Emberley, D. S. (1991). How stimulus direction determines the trajectory of the Mauthner-initiated escape response in a teleost fish. *J. Exp. Biol.* **161**, 469-487.
Fernandes, A. M., Fero, K., Arrenberg, A. B., Bergeron, S. A., Driever, W. and Burgess, H. A. (2012). Deep brain photoreceptors control light-seeking behavior in zebrafish larvae. *Curr. Biol. CB* **22**, 2042-2047.
Fetcho, J. R. (1986). The organization of the motoneurons innervating the axial musculature of vertebrates. I. Goldfish (*Carassius auratus*) and mudpuppies (*Necturus maculosus*). *J. Comp. Neurol.* **249**, 521-550.
Fleisch, V. C. and Neuhauss, S. C. F. (2006). Visual behavior in zebrafish. *Zebrafish* **3**, 191-201.
Fontaine, E., Lentink, D., Kranenbarg, S., Müller, U. K., van Leeuwen, J. L., Barr, A. H. and Burdick, J. W. (2008). Automated visual tracking for studying the ontogeny of zebrafish swimming. *J. Exp. Biol.* **211**, 1305-1316.
Gabriel, J. P., Mahmood, R., Kyriakatos, A., Söll, I., Hauptmann, G., Calabrese, R. L. and El Manira, A. (2009). Serotonergic modulation of locomotion in zebrafish: endogenous release and synaptic mechanisms. *J. Neurosci. Off. J. Soc. Neurosci.* **29**, 10387-10395.
Gahtan, E., Sankrithi, N., Campos, J. B. and O'Malley, D. M. (2002). Evidence for a widespread brain stem escape network in larval zebrafish. *J. Neurophysiol.* **87**, 608-614.
Gahtan, E., Tanger, P. and Baier, H. (2005). Visual prey capture in larval zebrafish is controlled by identified reticulospinal neurons downstream of the tectum. *J. Neurosci. Off. J. Soc. Neurosci.* **25**, 9294-9303.
Hirata, H., Ogino, K., Yamada, K., Leacock, S. and Harvey, R. J. (2013). Defective escape behavior in DEAH-box RNA helicase mutants improved by restoring glycine receptor expression. *J. Neurosci. Off. J. Soc. Neurosci.* **33**, 14638-14644.

Kimmel, C. B., Patterson, J. and Kimmel, R. O. (1974). The development and behavioral characteristics of the startle response in the zebra fish. *Dev. Psychobiol.* **7**, 47-60.
Kinkhabwala, A., Riley, M., Koyama, M., Monen, J., Satou, C., Kimura, Y., Higashijima, S.-I. and Fetcho, J. (2011). A structural and functional ground plan for neurons in the hindbrain of zebrafish. *Proc. Natl. Acad. Sci. USA* **108**, 1164-1169.
Knogler, L. D. and Drapeau, P. (2014). Sensory gating of an embryonic zebrafish interneuron during spontaneous motor behaviors. *Front. Neural Circuits* **8**, 121.
Kohashi, T. and Oda, Y. (2008). Initiation of Mauthner- or non-Mauthner-mediated fast escape evoked by different modes of sensory input. *J. Neurosci. Off. J. Soc. Neurosci.* **28**, 10641-10653.
Korn, H. and Faber, D. S. (2005). The Mauthner cell half a century later: a neurobiological model for decision-making? *Neuron* **47**, 13-28.
Lütcke, H., Murayama, M., Hahn, T., Margolis, D. J., Astori, S., zum Alten Borgloh, S. M., Göbel, W., Yang, Y., Tang, W., Kügler, S. et al. (2010). Optical recording of neuronal activity with a genetically-encoded calcium indicator in anesthetized and freely moving mice. *Front. Neural Circuits* **4**, 9.
Marder, E. and Abbott, L. F. (1995). Theory in motion. *Curr. Opin. Neurobiol.* **5**, 832-840.
Matthews, M., Trevarrow, B. and Matthews, J. (2002). A virtual tour of the Guide for zebrafish users. *Lab. Anim.* **31**, 34-40.
Mirat, O., Sternberg, J. R., Severi, K. E. and Wyart, C. (2013). ZebraZoom: an automated program for high-throughput behavioral analysis and categorization. *Front. Neural Circuits* **7**, 107.
Muto, A., Ohkura, M., Abe, G., Nakai, J. and Kawakami, K. (2013). Real-time visualization of neuronal activity during perception. *Curr. Biol. CB* **23**, 307-311.
Nair, A., Azatian, G. and McHenry, M. J. (2015). The kinematics of directional control in the fast start of zebrafish larvae. *J. Exp. Biol.* **218**, 3996-4004.
O'Malley, D. M., Zhou, Q. and Gahtan, E. (2003). Probing neural circuits in the zebrafish: a suite of optical techniques. *Methods* **30**, 49-63.
Parichy, D. M. (2015). Advancing biology through a deeper understanding of zebrafish ecology and evolution. *eLife* **4**, e05635.
Portugues, R. and Engert, F. (2009). The neural basis of visual behaviors in the larval zebrafish. *Curr. Opin. Neurobiol.* **19**, 644-647.
Severi, K. E., Portugues, R., Marques, J. C., O'Malley, D. M., Orger, M. B., Engert, F. (2014). Neural control and modulation of swimming speed in the larval zebrafish. *Neuron* **83**, 692-707.
Stewart, A. M., Grieco, F., Tegelenbosch, R. A. J., Kyzar, E. J., Nguyen, M., Kaluyeva, A., Song, C., Noldus, L. P. J. J. and Kalueff, A. V. (2015). A novel 3D method of locomotor analysis in adult zebrafish: Implications for automated detection of CNS drug-evoked phenotypes. *J. Neurosci. Methods* **255**, 66-74.
Stobb, M., Peterson, J. M., Mazzag, B. and Gahtan, E. (2012). Graph theoretical model of a sensorimotor connectome in zebrafish. *PLoS ONE* **7**, e37292.
Temizer, I., Donovan, J. C., Baier, H. and Semmelhack, J. L. (2015). A visual pathway for looming-evoked escape in larval zebrafish. *Curr. Biol. CB* **25**, 1823-1834.
Tinbergen, N. (1951). *The Study of Instinct*. Oxford: Clarendon Press.
Zelenin, P. V., Orlovsky, G. N. and Deliagina, T. G. (2007). Sensory-motor transformation by individual command neurons. *J. Neurosci. Off. J. Soc. Neurosci.* **27**, 1024-1032.
Zhu, L. and Weng, W. (2007). Catadioptric stereo-vision system for the real-time monitoring of 3D behavior in aquatic animals. *Physiol. Behav.* **91**, 106-119.